Available online at www.sciencedirect.com
ScienceDirect
Journal of Nuclear Materials 360 (2007) 255–264
journal of nuclear materials
www.elsevier.com/locate/jnucmat

Welding-induced mechanical properties in austenitic stainless steels before and after neutron irradiation

R. Stoenescu [a,b,*], R. Schäublin [b], D. Gavillet [a], N. Baluc [b]

[a] Laboratory for Materials Behaviour, Paul Scherrer Institute, 5232 Villigen PSI, Switzerland
[b] Fusion Technology Materials, CRPP–EPFL, Association EURATOM–Confederation Suisse, 5232 Villigen PSI, Switzerland

Received 9 January 2006; accepted 17 October 2006

Abstract

The effects of neutron irradiation on the mechanical properties of welded joints made of austenitic stainless steels have been investigated. The materials are welded AISI 304 and AISI 347, so-called test weld materials, irradiated with neutrons at 573 K to doses of 0.3 and 1.0 dpa. In addition, an AISI 304 from a decommissioned pressurised water reactor, so-called in-service material, which had accumulated a maximum dose of 0.35 dpa at about 573 K, was investigated. The mechanical properties of heat-affected zones and base materials were analysed before and after irradiation. Tensile parameters were determined at room temperature and at 573 K, for all materials and irradiation conditions. In the test weld materials it is found that radiation hardening is lower and loss of ductility is higher in the heat-affected zone than in the base material. In the in-service material radiation hardening is about the same in heat-affected zone and base material. After irradiation, deformation takes place by stacking faults and twins, at both room temperature and high temperature, contrary to un-irradiated materials, where deformation takes place by twinning at room temperature and by dislocation cells at high temperature. No defect free channels are observed.

1. Introduction

Changes in mechanical properties of neutron-irradiated austenitic stainless steels are the direct result of the irradiation-induced microstructure [1–5]. Mechanical properties of interest in this study include tensile strength and ductility. Numerous studies show an increase in the yield strength and a decrease of the uniform elongation in tensile tests, as the irradiation dose is increased. The ultimate tensile strength also increases to a lower extent. The data show that the highest hardening is obtained for irradiation and test temperatures of about 573 K [3].

The irradiation-induced increase in yield strength, referred to as radiation hardening, is usually assumed to be due to the formation of faulted interstitial loops, since they are the dominant microstructural features present in materials irradiated in light water reactors. The hardening can be estimated from the number density and the mean size of the loops, using the dispersed barrier hardening model [6–8] described in the discussion section of this article.

* Corresponding author. Present address: Institutt for Energiteknikk/OECD Halden Reactor Project, P.O. Box 173, N-1751 Halden, Norway. Tel.: +47 69 21 2357; fax: +47 69 21 2201.
E-mail address: ralucas@hrp.no (R. Stoenescu).

0022-3115/$ - see front matter © 2006 Elsevier B.V. All rights reserved.
doi:10.1016/j.jnucmat.2006.10.009

Hardening of austenitic stainless steels is accompanied by a loss of uniform elongation.

The deformation mechanism of irradiated and deformed austenitic stainless steels was extensively studied by transmission electron microscopy. Twinning was found to be the dominant deformation mode at room temperature [2,4,9–11]. At higher temperatures, around 573 K, dislocation channeling was observed [2,4,10,11]. The change in the deformation mechanism with temperature was explained by an increase in the stacking fault energy with temperature [12].

The goal of this study is to better understand the effects of neutron irradiation on the mechanical properties of heat-affected zones of welds made of three types of austenitic stainless steels. The deformation modes of the unirradiated and irradiated materials have been studied by transmission electron microscopy.

2. Experimental

The materials used in the present study are three types of austenitic stainless steels, the so-called test weld materials and in-service material. The so-called test weld materials are AISI 304 and AISI 347 welded by fusion and irradiated at a temperature of 573 K to a dose of 0.3 and 1.0 dpa. The so-called in-service material refers to a welded austenitic stainless steel type AISI 304 originating from the thermal shield of a decommissioned experimental pressurised water reactor (PWR) with a coolant temperature of about 573 K. Two plates with the same thermal history and different accumulated dose levels have been selected for the present study: Block A with doses between 1.3×10^{-5} and 1.3×10^{-4} dpa, and Block B with doses between 0.12 and 0.35 dpa. Details on materials and sample preparation from the heat-affected zone (HAZ) can be found in [13].

To asses the mechanical property changes induced in the HAZ due to the welding process and neutron irradiation, tensile tests were performed on specimens from the HAZ, at different distances from the fusion line (FL), and from the base material (BM), far away from the FL. Because of the small extension of the HAZ, tests were made within the framework of small specimen technology, using flat tensile specimens with the so-called Pirex geometry. The gage section dimensions are 5.5 mm length, 2.5 mm wide and about 0.35 mm thickness. The stress–strain relationship was determined at room temperature in air and at ~573 K in argon flow using a constant strain rate of $5 \times 10^{-4}\ s^{-1}$ in both unirradiated and irradiated conditions. Values of the different tensile test parameters, yield strength (YS), ultimate tensile strength (UTS) and uniform elongation (UE) were averaged from a minimum of ten measurements in the case of the unirradiated BMs and the error bars were determined from these values. For the HAZ as well as for the irradiated materials, only one specimen was available per condition. No specimens were available from the BM in the case of irradiated test weld materials.

The YS was measured at 0.2% plastic strain. The UTS corresponds to the maximum stress where necking is expected to start. The UE was measured at the highest stress level, i.e. at the onset of necking.

The microstructure after deformation has been studied by transmission electron microscopy (TEM). The observations were performed in a JEOL 2010 microscope operated at 200 kV.

3. Results and discussion

3.1. Mechanical properties

3.1.1. Test weld materials

Tensile tests were performed on specimens from the HAZ and BM of the unirradiated and irradiated materials at two deformation temperatures. The YS and UE were determined at 293 K and 573 K and values are reported in Table 1. It appears that the YS presents larger values in the HAZ as compared to the BM. The YS of both materials is observed to decrease with increasing temperature. The UE presents smaller values in HAZ as compared to the BM. The UE of both materials is observed to decrease with increasing temperature.

Radiation hardening is defined as the increase in YS of the irradiated material as compared to the unirradiated one. It is calculated as $\Delta\sigma = \sigma_{irr} - \sigma_{unirr}$ and it is plotted in Fig. 1(a) and (b) for AISI 304 and AISI 347, respectively, tested at 293 K. Data found in the literature for BMs such as AISI 304 L proton irradiated to 0.3 dpa at 520 K and neutron irradiated to 1.5 dpa at 550 K [14], as well as AISI 304 L proton irradiated at about 520 K up to 0.2 and 1.5 dpa [15] and tested at room temperature are also inserted in Fig. 1(a). The radiation hardening determined in the present study for the HAZ is observed to be smaller than the literature data found for the BM. Hardening increases with

Table 1
Tensile properties of unirradiated and irradiated AISI 304 and AISI 347 tested at 293 K and 573 K

Material		AISI 304				AISI 347			
		293 K		573 K		293 K		573 K	
		YS, MPa	UE, %	YS, MPa	UE, %	YS, MPa	UE, %	YS, MPa	UE, %
Unirradiated	1	349	42	276	13	345	49	282	14
	2	334	45	290	17	341	37	268	17
	3	380	57	328	16	375	40	292	17
	4	347	51	327	20	352	41	342	12
	BM	215	53	160	39	244	48	214	19
0.3 dpa	1	682	16	590	5	508	21	479	7
	2	605	21	502	4	571	16	457	8
	3	622	29	480	7	568	21	480	7
	4	613	25	488	8	574	29	446	6
1.0 dpa	1	683	14	460	5	645	13	481	10
	2	640	21	540	4	642	25	539	4
	3	634	24	430	10	620	23	514	6
	4	619	20	510	10	775	19	519	6
Deviation		±15%	±5%	±20%	±4%	±10	±6	±25%	±5%

Specimen 1: close to the fusion line, specimen 4: far away from the fusion line. BM: base material.

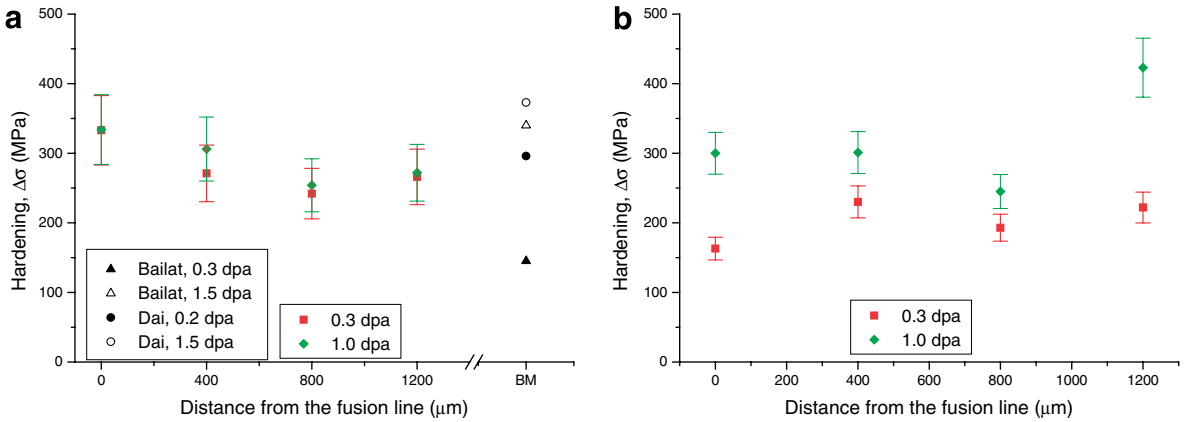

Fig. 1. Radiation hardening at 0.3 and 1.0 dpa as a function of the distance from the fusion line for (a) AISI 304 and (b) AISI 347 tested at 293 K. Data from the literature [14,15] for irradiated BM are included.

increasing irradiation dose, and this phenomenon is more marked in the case of AISI 347.

The loss of ductility is defined as the decrease in UE of the irradiated materials as compared to the unirradiated ones. It is calculated as $\Delta\varepsilon = \varepsilon_{unirr} - \varepsilon_{irr}$ and it is reported in Fig. 2(a) and (b) for AISI 304 and AISI 347, respectively, tested at 293 K, together with the literature data [14,15]. Loss of ductility is observed for both materials, whatever the distance from the FL and the temperature is. In the case of AISI 347 the data are more scattered. The loss of ductility determined in the present study for the HAZ is observed to be higher than the literature data found for BM.

The difference in the radiation hardening and loss of ductility in the HAZ as compared to the BM could be attributed to the different original microstructure of the two materials. The HAZ presents a different microchemistry, larger grain size, higher dislocation density and shows a ferritic interphase [13].

One of the contributions to the mechanical strength of a material is the dislocation–dislocation interaction. As the dislocation density in the HAZ was determined to be higher than in the BM [13],

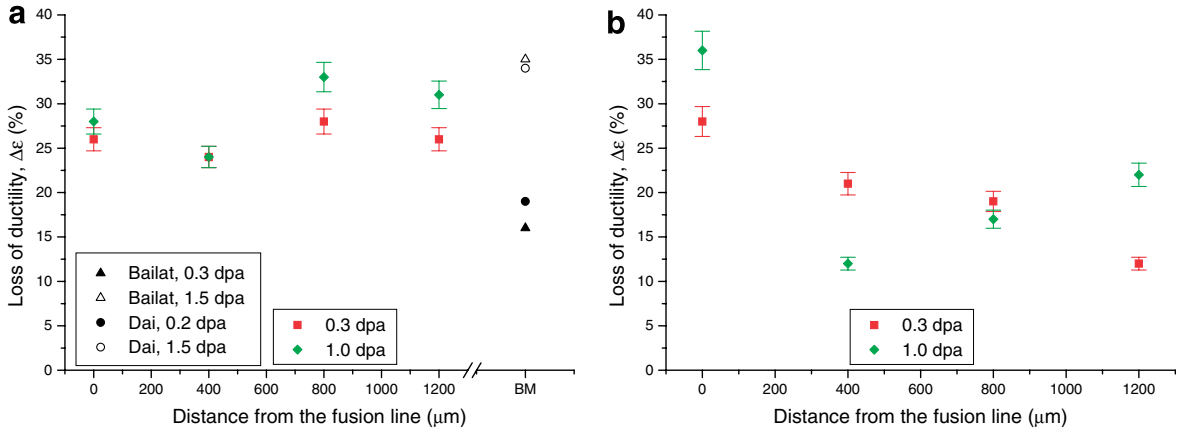

Fig. 2. Loss of ductility at 0.3 and 1.0 dpa as a function of the distance from the fusion line for (a) AISI 304 and (b) AISI 347 tested at 293 K. Data from the literature [14,15] for irradiated BM are included.

one may expect that the HAZ is harder than the BM. The following model is used [16]:

$$\Delta\sigma = M \cdot \alpha \cdot \mu \cdot b \cdot \sqrt{\rho}, \tag{1}$$

where M is the Taylor factor that relates to the shear stresses in a slip plane of a single crystal to the tensile stresses necessary to activate slip in a polycrystalline material and it is equal to 3.06 for fcc materials [17], α is a value that characterises the obstacle strength, taken equal to 0.2 in the case of dislocations [8], μ is the shear modulus, equal to 76.92 GPa for AISI 304 and 74.23 GPa for AISI 347, b is the modulus of the Burgers vector of the gliding dislocations, ρ is the dislocation density. The dislocations in an fcc structure have a Burgers vector of type $(a_0/2)\langle 1\,1\,0\rangle$ [18]. The lattice parameter a_0 was determined from diffraction patterns taken in TEM [13] to be (0.364 ± 0.014) nm for AISI 307 and (0.359 ± 0.014) nm for AISI 347, giving a Burgers vector modulus equal to 0.257 nm for and 0.253 nm, respectively.

The change in YS due to dislocation–dislocation interaction was calculated using Eq. (1) and the dislocation density values reported in [13]. The results are plotted in Fig. 3 for AISI 304 and AISI 347 tested at 293 K, as a function of the distance from the FL. The change in YS calculated as the difference between the experimental YS values for the HAZ and BM, determined from the stress–strain curves, $\Delta\sigma = \sigma_{HAZ} - \sigma_{BM}$, are also included in these graphs. For AISI 304 the calculated values follow the same trend as the experimental ones as a function of the distance from the FL, but differences exist between the absolute values. The trend is less clear for AISI 347. These differences can be attributed to the presence of other features, apart from

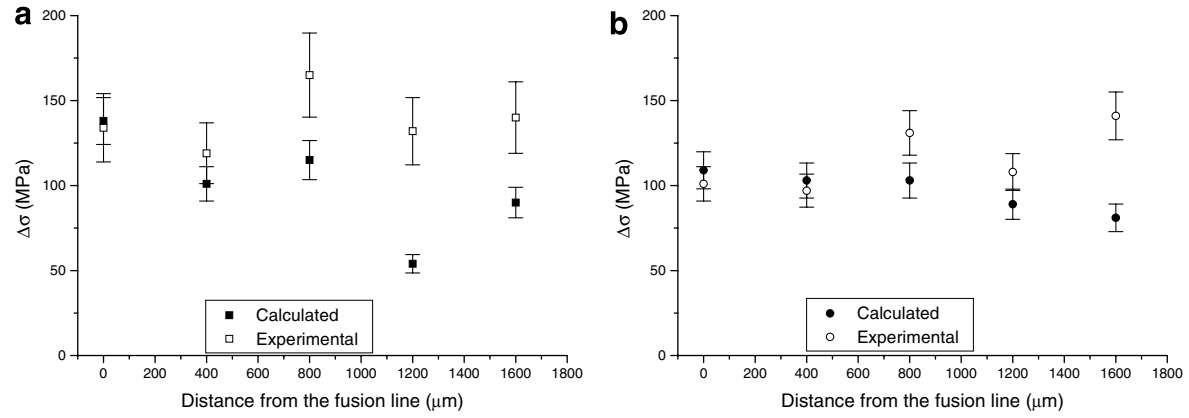

Fig. 3. Experimental (determined from stress–strain curves) and calculated (using Eq. (1)) yield strength due to dislocations as a function of the distance from the fusion line for (a) AISI 304 and (b) AISI 347 determined at 293 K.

dislocations, contributing to the YS. This could be due to the changes in the chemical composition of the HAZ, at local scale, due to the high temperatures reached during welding. The grain size is slightly larger in the HAZ with respect to the BM [13], which should yield a decrease in the YS of the HAZ with respect to that of the BM, according to the Hall–Petch relation [19], contrary to what is observed here. Another effect could come from the presence of the bcc ferritic interphase in the fcc austenitic matrix. In our study, the ferrite is intergranular and it could act as a strain hardener. The amount of ferrite in the HAZ is however small (3%) [13]. It should be noted that the variation of the ferrite–austenite ratio in welded duplex stainless steels was found to have no significant influence on the hardness [20].

In the case of irradiated materials, the changes in mechanical properties with respect to those of unirradiated ones are a direct consequence of the damage microstructure. Different models have been developed to explain the mechanical behaviour of irradiated materials from the microstructure evolution under irradiation. The dispersed barrier hardening model describes the increase in YS which is necessary to move a dislocation through a field of obstacles, in the present case the irradiation-induced defects. The YS increase, or radiation hardening, is given by [8]

$$\Delta\sigma_y = M \cdot \alpha \cdot \mu \cdot b \cdot (N \cdot d)^{1/2}, \tag{2}$$

where M is the Taylor factor as described above, α is a value that characterises the obstacle strength, μ is the shear modulus, b is the modulus of the Burgers vector of the gliding dislocations, as reported above, N is the number density and d is the mean size of obstacles, reported in [13]. The mean size of the total irradiation-induced defects consisting of black dots and Frank dislocation loops is calculated using the following mathematical formula:

$$d_{\text{mean}} = \frac{N_{\text{BD}} \cdot d_{\text{BD}} + N_{\text{FL}} \cdot d_{\text{FL}}}{N_{\text{total}}}, \tag{3}$$

where N_{BD} and N_{FL} is the number density of black dots and Frank dislocation loops, respectively; d_{BD} and d_{FL} is the mean size of black dots and Frank dislocation loops, respectively; N_{total} is the total number density of radiation-induced defects, namely black dots and Frank dislocation loops.

To determine the values for the obstacle strength α, the radiation hardening $\Delta\sigma_y$ is plotted as a function of $(N \cdot d)^{1/2}$, and the data is fitted with a straight line going through the origin, as there is no hardening in the case of unirradiated materials. The value of α was then determined from the slope of the straight line, m, using the following formula [21]:

$$\alpha = m/(M \cdot \mu \cdot b). \tag{4}$$

The radiation hardening was determined using an average value of YS calculated for the four specimens in the HAZ, using values from Table 1. In Fig. 4(a) and (b) radiation hardening is plotted against $(N \cdot d)^{1/2}$ for AISI 304 and AISI 347, respectively. The resulting α values, calculated using Eq. (4) and Fig. 4, are 0.14 for AISI 304 and 0.19 for AISI 347, respectively.

The obstacle strength values, α, usually range between 0.1 and 1, depending on the barrier type

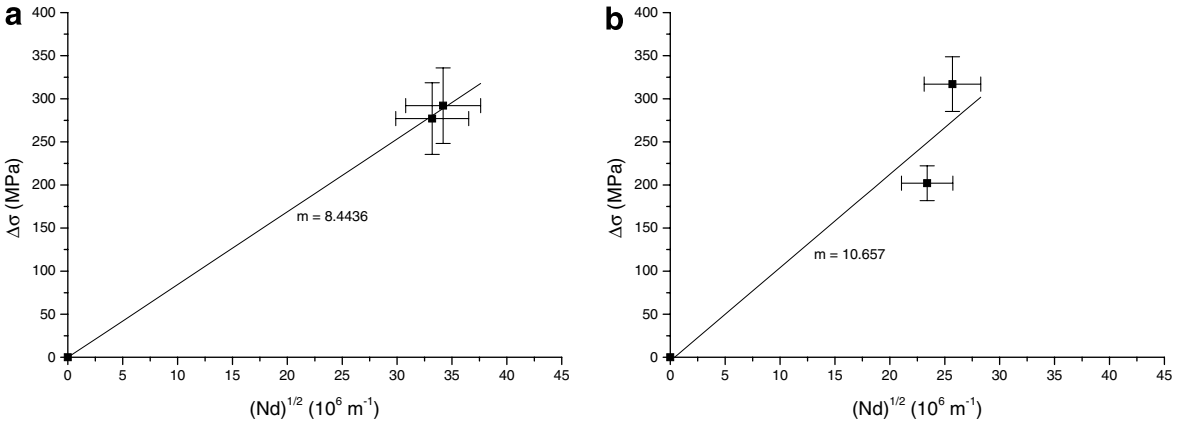

Fig. 4. Radiation hardening $\Delta\sigma$ versus the square root of the product of the defect cluster density and their mean size for (a) AISI 304 and (b) AISI 347 test weld materials irradiated at 573 K to doses of 0.3 and 1.0 dpa.

[8,14,16,22,23]. For weak obstacles, such as small loops and clusters, a value of 0.2 is usually found for α. According to the literature, for intermediate obstacles such as Frank dislocation loops, α is 0.33–0.4 [24]. The α values determined in the present study are small as compared to the literature ones. The radiation hardening has been calculated with Eq. (2), using the determined α values. The results are listed in Table 2, together with the radiation hardening experimentally determined from the stress–strain curves, for comparison. At 0.3 dpa the calculated radiation hardening shows higher values as compared to the experimentally determined ones, for both materials. At 1.0 dpa, the calculated radiation hardening shows lower values as compared to the experimentally determined values. These differences could be attributed to the fact that one cannot separate the contributions arising from different types of irradiation-induced defects.

Table 2
Experimental (determined from the stress–strain curves) and calculated (using Eq. (2)) radiation hardening values using fit-determined α values for the test materials irradiated at 573 K to 0.3 and 1.0 dpa

Material	Dose, dpa	Experimental $\Delta\sigma$, MPa	Calculated $\Delta\sigma$, MPa
AISI 304	0.3	277	282
$\alpha = 0.14$	1.0	292	290
AISI 347	0.3	202	256
$\alpha = 0.19$	1.0	317	281

3.1.2. In-service material

BR 304 in-service material shows a relatively different behaviour as compared to the test weld materials. Values of YS and UE as deduced from the stress–strain curves in the case of in-service material with different irradiation doses are summarised in Table 3. The YS presents slightly higher values in the HAZ as compared to the BM, at both deformation temperatures. The YS is lower at higher temperatures, for both BM and HAZ. The UE values are lower in the HAZ as compared to the BM, at both deformation temperatures. Radiation hardening has been calculated relative to the lowest dose, namely 1.3×10^{-5} dpa because of the lack of unirradiated material. Fig. 5(a) and (b) shows the radiation hardening variation with the

Table 3
Tensile properties of in-service material tested at 293 K and 573 K

	Dose, dpa	$T_{test} = 293$ K		$T_{test} = 573$ K		Dose, dpa	$T_{test} = 293$ K		$T_{test} = 573$ K	
		YS, MPa	UE, %	YS, MPa	UE, %		YS, MPa	UE, %	YS, MPa	UE, %
1	1.3×10^{-5}	386	47	335	20	0.12	523	34	–	–
2		420	40	335	19		520	31	414	17
3		–	–	331	19		500	33	390	12
4		416	42	319	18		514	31	345	–
5		–	–	267	17		510	31	378	–
6		405	46	300	18		610	24	404	14
7		440	42	278	22		473	36	390	–
BM		280	50	184	25		430	34	300	17
1	7.1×10^{-5}	413	46	375	17	0.23	537	32	414	–
2		418	44	366	18		527	31	436	14
3		434	–	357	19		552	30	473	15
4		403	48	350	20		553	30	410	13
5		374	47	255	22		494	34	424	14
6		381	48	308	25		490	32	–	–
7		368	52	302	25		467	36	–	–
BM		286	54	212	26		444	40	315	20
1	1.3×10^{-4}	452	36	352	17	0.35	518	28	491	13
2		–	–	345	19		550	23	512	16
3		431	34	354	21		568	21	490	14
4		460	42	340	20		570	24	488	–
5		439	39	333	22		582	30	456	12
6		446	44	364	20		593	29	435	–
7		414	41	286	25		504	34	442	18
BM		316	43	202	25		484	34	354	23

Specimen 1: close to the fusion line, specimen 7: far away from the fusion line. BM: base material.

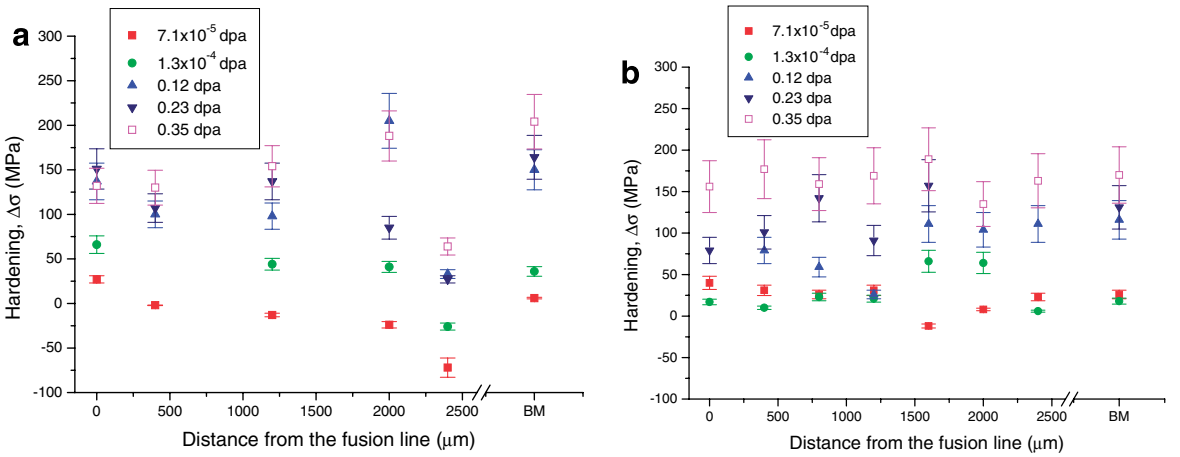

Fig. 5. Radiation hardening for the BR-304 in-service material tested at (a) 293 K and (b) 573 K.

irradiation dose and the distance from the FL determined at room temperature and at 573 K, respectively. Irradiation-induced hardening is observed for both material states (BM and HAZ), at both testing temperatures. For very low doses of the order of 10^{-5} dpa, softening is observed. Having in mind the smaller obstacle strength α values determined in the present study as compared to the values found in the literature, one may assume that a different hardening behaviour occurs at low doses. Nevertheless, further studies on austenitic stainless steels irradiated at very low doses are necessary to confirm this assumption. Hardening increases with increasing irradiation dose and it is found to be fairly constant along the FL, at both testing temperatures. At high temperatures the HAZ retains a slightly higher strength. The different behaviour of the HAZ and BM in the case of in-service material as compared to the test weld materials could be attributed to the different dose accumulation rate and possible stress relaxation in the in-service material due to much longer irradiation time.

3.2. Deformation microstructure

3.2.1. Unirradiated materials

TEM observations performed on deformed unirradiated materials revealed that at room temperature twinning contributes significantly to the deformation process (Fig. 6(a)). The twins are in $\{111\}$ planes along $\langle 110\rangle$ directions, as it is deduced from the diffraction pattern inserted in Fig. 6(a). At high temperature, perfect dislocation motion prevails (Fig. 6(b)). There is no difference between the deformation mechanism taking place in the HAZ and the one operating in the BM, for all the studied materials, AISI 304, AISI 347, BR 304.

3.2.2. Irradiated materials

The deformation-induced microstructure of irradiated materials depends to a large extent on the microstructure that developed under irradiation. In the present study it was found that, in the case of the in-service material, deformation takes place mainly by twinning at both testing temperatures for both BM and HAZ. The deformation of both AISI 304 and AISI 347 test weld materials irradiated up to 0.3 dpa (Fig. 7) or 1.0 dpa (Fig. 8) takes place by the formation of a mixture of twins and stacking faults, at both deformation temperatures, whatever the distance from the FL is. The change in deformation mechanism at high temperatures in the irradiated materials is due to higher stress levels necessary to produce plastic deformation. The twins found in the deformation microstructure were studied in more detail, also in specimens taken far away from the necking region. Fig. 9 shows weak-beam dark-field images of a twin under two different diffraction conditions, close to a $\langle 110\rangle$ zone axis. In Fig. 9(a), taken with a $\{200\}$ diffraction vector, the twin appears free of defects. However, using a $\{111\}$ diffraction vector, defects are clearly observed inside of the twin (Fig. 9(b)).

The deformation mechanism of irradiated pure metals and austenitic stainless steels has been widely studied [15,17,24–31]. However, the deformation mechanism of irradiated austenitic stainless steels

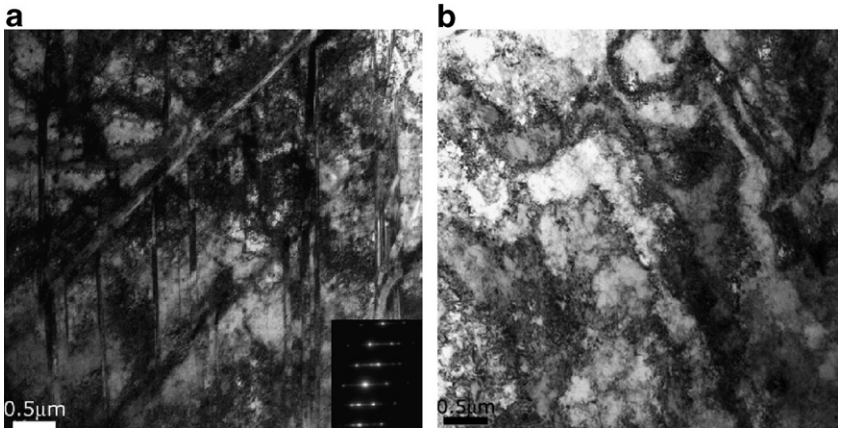

Fig. 6. Bright-field TEM images of AISI 347 tested at (a) 293 K and (b) 573 K.

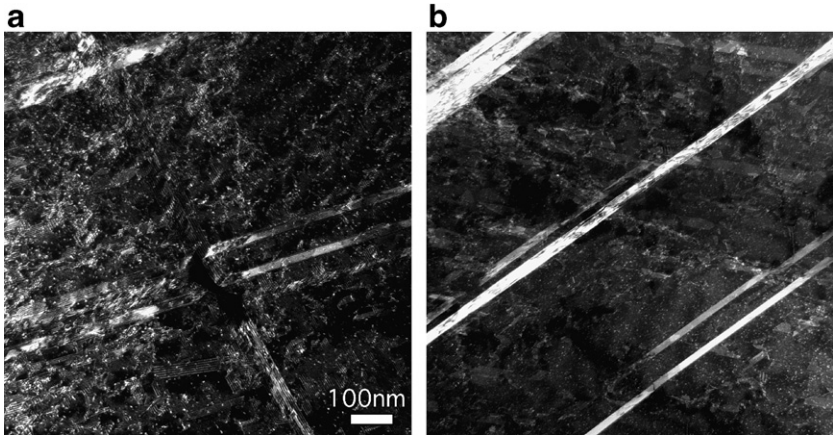

Fig. 7. Bright-field TEM images of 0.3 dpa AISI 304 close to the fusion line deformed at (a) 293 K and (b) 573 K.

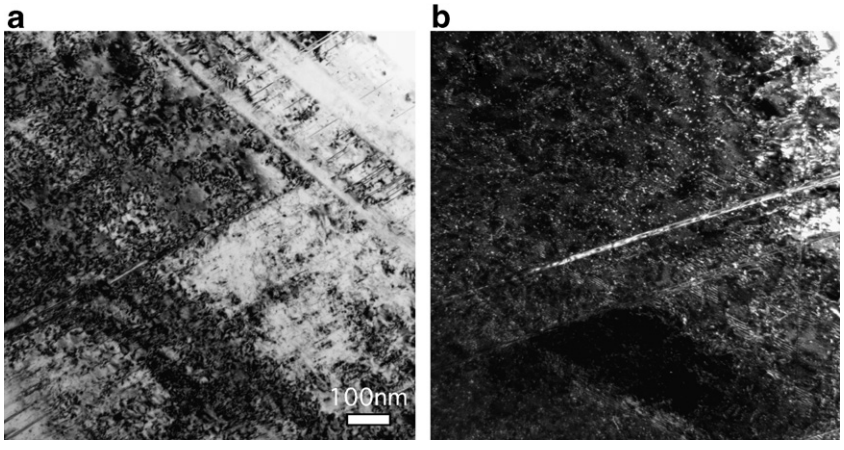

Fig. 8. Bright-field TEM images of 1.0 dpa AISI 347: (a) far away from the fusion line deformed at 293 K and (b) close to the fusion line deformed at 573 K.

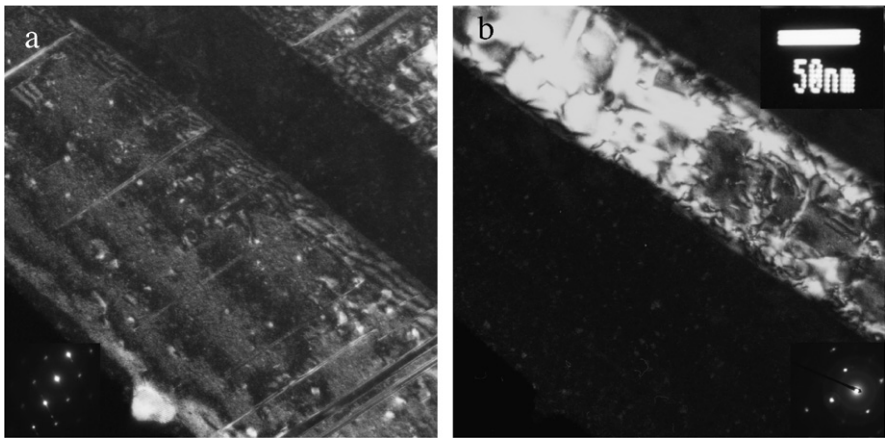

Fig. 9. Weak-beam dark-field TEM images of AISI 304 close to the fusion line irradiated up to 1.0 dpa and deformed at 293 K. Twin imaged close to a {1 1 0} zone axis using a (a) {2 0 0} and (b) {1 1 1} diffraction vector, as shown by the diffraction pattern inserted at one of the lower corner of each figure.

is rather controversial. The results indicate that the deformation proceeds by formation of defect free channels [14,24], stacking faults and twins [17,25,26] or by a combination of those [27]. Defect free channels, as observed in deformed, irradiated pure metals such as Cu or Pd [28], appear to be due to the sweeping, absorption and/or destruction of the irradiation-induced defects by moving dislocations. Once the irradiation-induced defects have been destroyed or weakened by the passage of a first dislocation, subsequent dislocations that stem from the same source, may propagate more easily than in the surroundings that still contain the original defect microstructure. It should be noted that Byun and Farrell [29] concluded that channeled deformation occurs under high stresses, in both unirradiated and irradiated materials. In other studies concerning channeling, the authors concluded that the channels are not completely free of defects, but contain a remnant density of Frank dislocation loops [11,29,30].

No defect free channels have been observed in the present study in any of the materials, at any testing temperature. This can be explained using the mechanism proposed by Song et al. [25] or Niewczas and Saada [31].

Song et al. [25] suggested that the formation of twins in irradiated fcc materials with low stacking fault energy occurs by the unfaulting of Frank loops, following the intersection of more than one dislocation with a Frank loop. Two partials are formed after a first dislocation interacts with the loop. With more dislocations intersecting the loop, the partial dislocations are further separated. In materials with low stacking fault energy the unfaulting of the loop depends on the local shear stress. Because the attraction force between the two partials is large, a high energy is necessary to separate them. The low stacking fault energy in stainless steels facilitates the extension of the stacking faults and the formation of twins.

Niewczas and Saada [31] explained the twin nucleation from Frank loops by Shockley partial dislocations bounding a stacking fault. Depending upon the position of the primary dislocation with respect to the twinning dislocation, four configurations of twinning sources can be considered. The growth of the twin proceeds by the motion of a Shockley partial around the primary poles. The sessile Frank jog can act as stress barrier for the twinning source. If two twinning dislocations pass the sessile jog simultaneously, the stress barrier is reduced to zero. If only one dislocation passes, the twinning dislocation may get stack at the Frank jog, producing a block of undeformed matrix inside the twinned material.

4. Conclusions

The effects of neutron irradiation on the mechanical properties of welded joints made of austenitic stainless steels have been investigated. The materials were AISI 304 and AISI 347 welded by fusion welding process and irradiated with neutrons at 573 K to 0.3 and 1.0 dpa. An AISI 304 type austenitic stainless steel from a decommissioned water reactor

(in-service material), which had accumulated a maximum dose of 0.3 dpa at about 573 K, was also investigated.

Studies of the mechanical properties of HAZs and BMs have been performed before and after irradiation, and the following results were obtained. The HAZ of all studied materials shows higher strength and lower ductility as compared to the BM, at both testing temperatures (293 K and 573 K). Neutron irradiation induces hardening and loss of ductility in all materials, at both testing temperatures. Radiation hardening presents lower values for the HAZ as compared to the BM, while loss of ductility is larger for the HAZ with respect to the BM, in the case of the test weld materials. In the case of in-service material radiation hardening is similar in the HAZ and BM.

Investigation of the deformed specimens revealed that in the unirradiated materials tested at room temperature, twinning is the dominant deformation mode, while dislocation glide prevails at high temperature. The deformation mode does not depend on the distance from the FL. In irradiated materials the deformation microstructure consists of a large amount of twins and stacking faults, independently on the position from the FL, the deformation temperature and the dose. Based on the presence of radiation-induced defects inside the twins, it was concluded that no defect free channels form in austenitic stainless steels under deformation, at least under the conditions investigated here.

Acknowledgements

R. Stoenescu would like to thank Drs P. Veyssière and J.T. Busby for fruitful discussions. This work was performed with the financial support of the European Commission, EURATOM FP5, contract number FIKS–CT–2000–00103, INTERWELD.

References

[1] T.S. Byun, K. Farrell, E.H. Lee, J.D. Hunn, L.K. Mansur, J. Nucl. Mater. 298 (2001) 269.
[2] N. Hashimoto, S.J. Zinkle, A.F. Rowcliffe, J.P. Robertson, S. Jitsukawa, J. Nucl. Mater. 283–287 (2000) 528.
[3] J.E. Pawel, A.F. Rowcliffe, D.J. Alexander, M.L. Grossbeck, K. Shiba, J. Nucl. Mater. 233–237 (1996) 202.
[4] J.L. Brimhall, J.I. Cole, S.M. Bruemmer, Scr. Metall. Mater. 30 (1994) 1473.
[5] T. Onchi, K. Dohi, N. Soneda, J.R. Cowan, R.J. Scowen, M.L. Castano, J. Nucl. Mater. 320 (2003) 194.
[6] S.J. Zinkle, Y. Matsukawa, J. Nucl. Mater. 329–333 (2004) 88.
[7] A.L. Bement Jr., in: W.C. Leslie (Ed.), Proceedings of Second International Conference on Strength of Metals and Alloys, vol. II, ASM, Metals Park, OH, 1970, p. 693.
[8] G.E. Lucas, J. Nucl. Mater. 206 (1993) 287.
[9] T.S. Byun, K. Farrell, E.H. Lee, J.D. Hunn, L.K. Mansur, J. Nucl. Mater. 298 (2001) 269.
[10] M. Victoria, N. Baluc, C. Bailat, Y. Dai, M.I. Luppo, R. Schäublin, B.N. Singh, J. Nucl. Mater. 276 (2000) 114.
[11] K. Farrell, T.S. Byun, N. Hashimoto, J. Nucl. Mater. 335 (2004) 471.
[12] R.E. Schramm, R.P. Reed, Metall. Trans. A 6 (1975) 1345.
[13] R. Stoenescu, R. Schäublin, D. Gavillet, N. Baluc, J. Nucl. Mater., in press, doi:10.1016/j.jnucmat.2006.10.007.
[14] C. Bailat, F. Gröschel, M. Victoria, J. Nucl. Mater. 276 (2000) 283.
[15] Y. Dai, X. Jia, J.C. Chen, W.F. Sommer, M. Victoria, G.S. Bauer, J. Nucl. Mater. 296 (2001) 174.
[16] A.S. Krausz, K. Krausz (Eds.), Unified Constitutive Laws of Plastic Deformation, Academic Press Inc., 1996.
[17] X. Jia, Doctoral thesis 2702, EPFL, 2003.
[18] D. Hull, D.J. Bacon, Introduction to Dislocations, Pergamon, 1984.
[19] E.O. Hall, Proc. Phys. Soc. B 64 (1951) 747.
[20] V. Muthupandi, P. Bala Srinivasan, S.K. Seshadri, S. Sundaresan, Mater. Sci. Eng. A 358 (2003) 9.
[21] N. Baluc, Y. Dai, M. Victoria, in: J.B. Bilde-Sørensen, et al. (Ed.), Proceedings of 20th Risø International Symposium on Materials Science, 1999, p. 245.
[22] S.J. Zinkle, Y. Matsukawa, J. Nucl. Mater. 329–333 (2004) 88.
[23] R. Schäublin, D. Gelles, M. Victoria, J. Nucl. Mater. 307–311 (2002) 197.
[24] G.S. Was, J.T. Busby, Philos. Mag. 85 (2005) 443.
[25] S.G. Song, J.I. Cole, S.M. Bruemmer, Acta Mater. 45 (1997) 501.
[26] T.S. Byun, Acta Mater. 51 (2003) 3063.
[27] E.H. Lee, T.S. Byun, J.D. Hunn, M.H. Yoo, K. Farrell, L.K. Mansur, Acta Mater. 49 (2001) 3269.
[28] Y. Dai, Doctoral thesis 1388, EPFL, 1995.
[29] T.S. Byun, K. Farrell, Acta Mater. 52 (2004) 1597.
[30] E.H. Lee, T.S. Byun, J.D. Hunn, K. Farrell, L.K. Mansur, J. Nucl. Mater. 296 (2001) 183.
[31] M. Niewczas, G. Saada, Philos. Mag. A 82 (2002) 167.